Yeast
Yeast 2003; **20**: 53–67.
Published online in Wiley InterScience (www.interscience.wiley.com). **DOI:** 10.1002/yea.931

Yeast Functional Analysis Report

Automated screening in environmental arrays allows analysis of quantitative phenotypic profiles in *Saccharomyces cerevisiae*

Jonas Warringer and Anders Blomberg*
Department of Cell and Molecular Biology, Lundberg Laboratory, Göteborg University, Medicinaregatan 9c, 413 90 Göteborg, Sweden

**Correspondence to:*
Anders Blomberg, Department of Cell and Molecular Biology, Lundberg Laboratory, Göteborg University, Medicinaregatan 9c, 413 90 Göteborg, Sweden.
E-mail: anders.blomberg@gmm.gu.se

Received: 16 March 2002
Accepted: 16 September 2002

Abstract

A methodology for large-scale automated phenotypic profiling utilizing quantitative changes in yeast growth has been tested and applied to the analysis of some commonly used laboratory strains. This yeast-adjusted methodology is based on microcultivation in 350 μl liquid medium, where growth is frequently optically recorded, followed by automated extraction of relevant variables from obtained growth curves. We report that cultivation at this micro-scale displayed overall growth features and protein expression pattern highly similar to growth in well aerated medium-scale (10 ml) culture. However, differences were also encountered, mainly relating to the respiratory potential and the production of stress-induced proteins. Quantitative phenotypic profiles for the laboratory yeast strains W303, FY1679 and CEN-PK.2 were screened for in environmental arrays, including 98 different conditions composed of low, medium and high concentrations of 33 growth inhibitors. We introduce the concepts phenotypic index$_{rate}$ and phenotypic index$_{stationary}$, which relate to changes in rate of growth and the stationary phase optical density increment, respectively, in a particular environment relative a reference strain. The laboratory strains presented selective phenotypic profiles in both phenotypic indexes and the two features appeared in many cases to be independent characteristics. We propose the utilization of this methodology in large-scale screening of the complete collection of yeast deletion mutants. Copyright © 2002 John Wiley & Sons, Ltd.

Keywords: phenotypic profiling; microcultivation; yeast strains; 2D–PAGE; growth inhibitors

Introduction

Even for well-studied organisms such as *Saccharomyces cerevisiae*, the function of the majority of proteins encoded by the genome has not been experimentally determined. Protein function can be described at different levels of resolution and in this respect initiatives like the Gene Ontology Project have taken an important step to a more uniform treatment of functional annotations (Dwight *et al*., 2002; Lewis *et al*., 2000). At the highest level of resolution, it proposes the use of the term 'molecular function', which is a biochemical functional description, e.g. NAD^+-dependent sn-glycerol 3-phosphate dehydrogenase. However, for many of the database annotations function is described at the next level of functional resolution — the biological process/cellular role. Here can be found data obtained from classical forward genetic analysis, where mutants with certain phenotypes have been isolated, e.g. cdc mutants defective in functions related to the cell division cycle or gal mutants impaired in the utilization of the carbon source galactose. Phenotypic screens are thus frequently a first important step to the functional characterization of genes/proteins.

In large-scale screens for mutant phenotypes, qualitative analysis is the rule. Qualitative phenotypic analyses on agar plates have been applied to a large set of yeast mutants within the EUROFAN II project and there have lately been several reports describing analysis of deletion mutants under a limited number of growth conditions (Bilsland *et al*., 1998; Chan *et al*., 2000; Hajji *et al*., 1999; Lafuente and Gancedo, 1999; Rodriguez-Navarro *et al*., 1999; Wysocki *et al*., 1999; Zuniga *et al*., 1999). However, wider screens encompassing hundreds of chemicals affecting diverse cellular features have also been attempted and, by applying robotics and screens on agar plates, hundreds of mutants have been investigated (Rieger *et al*., 1999a,b, 1997; Ross-Macdonald *et al*., 1999). These analyses have provided novel insight into the cellular role of quite a number of genes for which no functional information was available earlier. Maybe most importantly, it was clearly shown that phenotypic effects were observed to a similar degree in mutants deleted for genes that are presently functionally unknown, compared to mutants deleted for functionally known genes (Bianchi *et al*., 2001). Thus, the functionally unknown genes/proteins appear to be of equal functional importance to cellular physiology as their already characterized counterparts. However, in screens on solid media, the criteria for identifying a certain phenotype is usually based on visual inspection and subsequent subjective evaluation of effects. In some cases the size of the colonies or the thickness of the cell paste has been used in these subjective scores (Ross-Macdonald *et al*., 1999). A fundamental problem in the interpretation of the colony size on an agar plate after a certain period of incubation is that an altered size is the composite of change in the length of lag phase, change in rate of growth and change in growth yield, while the physiological consequence of a mutation can be envisaged to occur on either one or on a combination of these different growth features. In addition, a technical problem with screens on agar is the non-consistent growth of colonies on plates, which depends on a number of factors (number of colonies per surface area, drying out effects, etc.), and confirmation experiments usually have to be performed.

An even more serious problem is that qualitative screens will in many cases not be able to encapsulate the full phenotypic character of the mutant (Ross-Macdonald *et al*., 1999; Winzeler *et al*., 1999). Thatcher *et al*. (1998) convincingly report on the important contribution to marginal fitness of non-essential genes in yeast. This was demonstrated by competition experiments for batch cultures of mixed populations of wild-type and the corresponding mutant that are serially transferred; a majority of randomly chosen mutants was shown to adhere to the marginal benefit hypothesis. It is also clear from fundamental considerations that for a large number of gene deletions we should expect minor quantitative changes in growth, in particular where compensatory mechanisms can be expected (Oliver, 1997). Minor differences in fitness between strains have also been analysed in well-controlled continuous cultivation, where competition is followed for many generations (Baganz *et al*., 1998). A technology with great potential in quantitative analysis of fitness of many mutants in parallel is large-scale screens utilizing 'bar-coded' deletion mutants (Giaever *et al*., 2002; Steinmetz *et al*., 2002; Winzeler *et al*., 1999). This powerful approach, where simultaneous screens for pooled populations of mutants are performed with utilization of specialized DNA microarrays, also possesses some fundamental problems: (a) inhibition between strains; (b) complementation of some strains by lysis of certain cell populations; (c) relatively large variation in the data; (d) low growth rates difficult to record; and (e) restriction of the number of analyses to be performed, due to economic considerations. The most serious concern might be the positive and negative interactions between mixed strains that will be an inherent consequence of this experimental set-up. The overall aim in phenotypic analysis is to acquire information about growth properties of particular mutants that would indicate physiological consequences from gene deletions. Instead this experimental set-up with pooled populations measures the relative fitness between strains, which will be a composite of features such as time of adaptation and rate and efficiency of growth, but will also relate to the type and amount of inhibitory substances produced or the competition between strains for available nutrients. The consequence is that the competition design measures well the relative fitness of strains and will provide valuable information about analysis of population genetics and evolutionary processes, e.g. the relation between protein dispensability and evolutionary rate (Hirsh and Fraser, 2001). However, it

might not be equally well-suited for the analysis of strain-specific phenotypic traits that are to be interpreted as gene-by-environment interactions linked to features of cellular physiology. This statement is further supported by the lack of correlation between the observed relative fitness and growth features, such as doubling time or stationary-phase cell density, in the analysis of drug resistance in populations of *Candida albicans* (Cowen *et al*., 2001).

In an attempt to provide consistent and more easily interpreted quantitative phenotypic information, we here present and evaluate a procedure based on microscale liquid cultivation of yeast in an automated microplate system, combined with automation of the subsequent data analysis. The system provides high resolution and can distinguish between marginal effects in growth rate and stationary phase OD increments. It is proposed that the system described can successfully be used for large-scale projects, where quantitative changes in growth phenotypes are screened for during a wide variety of growth conditions for all viable yeast deletion mutants.

Materials and methods

Strains

The haploid strains used in this study are yWJN-001-1B *(matα, ura 3-1, leu 2-3, 112, trp 1-1, his 3-11, 15, ade 2-1, can1-100*; derived from the diploid W303), yFJN001-1D *(matα, ura 3-52, trp 1-63, leu 2-3 his 3-200*; derived from the diploid FY1679), yCJN001-1B *(matα, ura 3-52, leu 2-3,112, trp 1-289, his 3-1*; derived from the diploid CEN-PK.2) (Rogowska-Wrzesinska *et al*., 2001), where all diploids were provided by the EUROSCARF yeast stock centre, and *YPH500 (matα, ura3-52, lys2-801amber, trp1-deltaG3, his3-delta200, leu2-delta1, ade2-101ocre)* (Brachmann *et al*., 1998). Strains were long-term stored at −80 °C in 20% (w/v) glycerol solution and pre-experimentally stored at +4 °C for a maximum of 2 weeks (agar plates) or 5 months (agar slopes).

Media and growth conditions

The synthetic defined medium (SD), buffered with succinate to pH 5.8, was used (Rogowska-Wrzesinska *et al*., 2001) and supplemented with 20 mg/l adenine, 20 mg/l uracil, 20 mg/l tryptophan, 20 mg/l histidine and 100 mg/l leucine.

Growth in microplates was automatically recorded using a Bioscreen analyser C (Thermic Labsystems Oy, Finland). The optical density was measured using a wide band (450–580 nm) filter to reduce the contribution to the reading from the medium. Incubation were kept at 30.0 °C, ±0.1 °C (10 min preheating time). The plates were subjected to shaking at the highest shaking intensity with 60 s of shaking every other minute. OD measurements were taken every 20 min during a 24 h period. This time-span allows for maximum throughput while still allowing most yeast cells (with a doubling time <4.5–5 h) to reach stationary phase. Strains were run in duplicates (separated by day of the run and plate position).

Inoculation cultures were taken from cultures that had been inoculated from loop-fulls of cells from agar plates and incubated overnight (approximately 18 h) at 30 °C on a rotator in 5 ml SD medium in 15 ml plastic test tubes (Falcon). Precultures were harvested by centrifugation, washed in 5 ml sterile MilliQ water and, for the automated growth measurements in the Bioscreen C, inoculated to OD 0.10–0.15 (OD value obtained in the Bioscreen C; OD in the Bioscreen C is measured relative air and the average OD of non-inoculated wells with SD medium is 0.067) in fresh SD media in 100-well microplates (denoted honeycomb plates by the supplier). Each well contains 350 μl medium.

For manual growth measurements in E-flasks pre-cultures were treated as described above and inoculated to OD 0.07 in 125 ml E-flasks, 10 ml medium in each culture. The E-flasks were kept at 30 °C ± 1 °C and the cultures were subjected to orbital shaking at high intensity (200 rpm). Optical density measurements were manually performed at 0.5–1 h time intervals at 610 nm in a Novospec II spectrophotometer (Pharmacia Biotech) and the samples diluted at OD values above 0.35. Three measurements were taken during the later stages of the stationary phase.

Inhibitors

All inhibitors were obtained at the highest available grade (Sigma Aldrich). Concentrations were as follows: methylviologen (paraquat), 167, 84 and 42 μg/ml; menadione, 0.1, 0.03

and 0.006 mM; benomyl, 50, 10 and 1 μg/ml; ethanol, 6, 5 and 4%; 4-NQO, 0.007, 0.0035 and 0.001 μg/ml; cycloheximide, 0.03, 0.01 and 0.001 μg/ml; hydroxyurea, 15, 6 and 2 mg/ml; tunicamycin, 2, 0.5 and 0.1 μg/ml; hygromycin B, 0.25, 0.1 and 0.025 mg/ml; rapamycin, 0.05, 0.025 and 0.01 μg/ml; 1,10 phenanthroline, 0.01, 0.005 and 0.0025 mM; caffeine, 1.5, 1 and 0.5 mg/ml; compound 48/80, 10, 5 and 2.5 μg/ml; calcofluor white, 2, 0.4 and 0.08 mg/ml; DNP, 0.2, 0.1 and 0.05 mg/ml; SDS, 0.01, 0.0075 and 0.005%; cytochalasin D, 5, 2.5 and 1 μg/ml, trifluoperazine, 12.5, 10 and 7.5 μM; canavanine, 10, 5 and 1 μg/ml; diamide, 1, 0.75 and 0.5 mM; $CdCl_2$ 5 and 2 μg/ml; neomycin sulphate, 35, 18 and 9 mM; $CaCl_2$ 500, 150 and 50 mM; NaCl, 1.0, 0.75 and 0.5 mM; sorbitol, 1, 0.75 and 0.5 mM; EGTA, 30, 15, 7.5 mM; G418, 525, 262.5 and 131.25 μg/ml; Brefeldin A, 890, 445 and 100 μM; AT-3, 175, 131.25 and 87.5 mM; camptothecin, 120, 90 and 60 μg/ml; 2,3-DPG, 12.5, 6.25 and 1 mM; ethidiumbromide, 180, 90 and 45 μg/ml; and vanadium, 6 and 3.75 mM).

Analysis of growth data

Data was exported from the microplate reader in AscII format and further processed in Excel (Microsoft Office 98) by an automated procedure implemented in Visual Basic (the macro is available upon request). The observed OD (OD_{obs}) values, from which the average blank (OD recorded with water) value of 0.067 has been subtracted, were converted to corrected OD (OD_{cor}); (correcting for the non-linearity at higher cell densities) using the formula $OD_{cor} = OD_{obs} + 0.449(OD_{obs})^2 + 0.191(OD_{obs})^3$. A smoothing procedure was applied to remove negative slopes along the growth curve; if any calculated slope between two consecutive OD measurements was negative, the latter of the consecutive data values was adjusted to equal the higher. All subsequent calculations were performed on the calibrated and smoothed growth data.

Estimation of lag phase

OD_{cor} values were $\log_{10}$-transformed. An initial OD was calculated as the mean of the initial six measurements (corresponding to the first 2 h of growth, the time chosen as the minimum lag phase observed from visual inspection of 600 growth curves). A slope was calculated from every eight consecutive data values (corresponding to a time span of 2.5 h) along the curve. An intercept between every slope and a straight line corresponding to the initial OD was calculated. Values exceeding 18 h were discarded. A mean of the two highest of the calculated intercepts was taken as the lag phase.

Estimation of doubling time

OD_{cor} values were $\log_{10}$ transformed. A slope was calculated between every third consecutive measurement for the whole growth curve. Slopes of more than 0.16 (chosen *ad hoc* as representing the fastest observed growth for cells grown in rich medium) were discarded. Of the seven highest slopes, the highest two were discarded to provide a safety margin, and a mean was calculated for the following five. The doubling time was calculated as $\log_{10}$ 2 divided by the mean of the slopes.

Estimation of stationary phase OD increment

End OD was calculated as the mean of the OD_{cor} measurements corresponding to the six last time points. If the standard deviation was higher than 2% of the mean (chosen *ad hoc* as the approximate threshold for a true plateau in the stationary phase from manual observation of 600 growth curves) the mean was not considered to represent a culture that had reached a stationary phase during the 24 h measurement period and no OD increment value was calculated from that curve. The initial OD was calculated in the same way as for the lag phase, and the difference between end OD and initial OD was taken as the stationary phase OD increment.

Calculation of phenotypic index

The phenotypic index for a strain s is here defined as a relative value to some reference strain rf. phenotypic $index_{rate}$: for each of the growth curves the specific growth rate constant, μ, was calculated ($\mu = \log 2/D$, where D stands for doubling time). The μ obtained in one particular growth condition i, μi, was divided by the μ obtained during growth in control medium c, μc, to obtain the environmental coefficient of rate of growth ($EC_{rate,i} = \mu i/\mu c$). The rate component of the phenotypic index, phenotypic $index_{rate}$, is defined as the $EC_{rate,i}$ ratio

between the strain s and the reference strain rf (phenotypic $\text{index}_{\text{rate,i,s}} = \text{EC}_{\text{rate,i,s}}/\text{EC}_{\text{rate,i,rf}}$). Phenotypic $\text{index}_{\text{stationary}}$: the stationary phase OD increment obtained in one particular growth condition i, ΔODi, was divided by the stationary phase OD increment obtained during growth in the control medium c, ΔODc, to obtain the environmental coefficient of stationary phase OD increment ($\text{EC}_{\text{stationary,i}} = \Delta\text{ODi}/\Delta\text{ODc}$). The stationary phase OD increment component of the phenotypic index, phenotypic $\text{index}_{\text{stationary}}$, is defined as the $\text{EC}_{\text{stationary,i}}$ ratio between the strain s and the reference strain rf (phenotypic $\text{index}_{\text{stationary,i,s}} = \text{EC}_{\text{stationary,i,s}}/\text{EC}_{\text{stationary,i,rf}}$). Thus, either a phenotypic $\text{index}_{\text{rate,i,s}}$ or phenotypic $\text{index}_{\text{stationary,i,s}}$ of less than one (1) would be indicative of a greater defect on growth in condition i for the strain under study compared to the reference strain.

High resolution IPG/2D–PAGE

Strains were grown to mid-exponential phase ($7–8 \times 10^6$ cells/ml in Bioscreen Analyzer C, 5×10^6 for manual growth) and labelled with 0.14 μCi [^{35}S]-methionine for 30 min. Growth was terminated by transferring cultures to microtubes on ice. Subsequent preparation of cell extracts and determination of incorporated radioactivity was essentially performed as previously reported (Blomberg *et al*., 1995), with the exceptions that during extract preparation the volumes and the amount of glass beads were halved for the microcultivated samples. Isoelectric focusing and second-dimensional separation, as well as image analysis, were performed as earlier reported (Norbeck and Blomberg, 1997). Identifications of proteins were accomplished using the reference 2D pattern (**http://yeast-2dpage.gmm.gu.se**).

Results

Optical recording of yeast growth

A technical challenge in the automated recording of yeast growth by optical density (OD) measurement is the non-linear response at higher cell densities. Yeast cultures should thus ideally be diluted at higher OD values, however, that is not feasible in a high-throughput set-up. A procedure to correct for the non-linearity of OD measurements for bacterial cultures has been presented (Dalgaard *et al*., 1994). Similarly, we found a correlation between the observed OD (OD_{obs}) of yeast cultures measured in the microplates of non-diluted cultures and the OD estimated from measuring diluted samples (OD_{dil}) (Figure 1A). Most importantly, this correlation appeared to be generally applicable, since we could not see any significant discrepancies relating to either growth phase (exponential vs. stationary) or strain (W303, FY 1679 and CEN-PK2) (Figure 1A). Independence of the strain/species and growth phase on the correlation function was also reported for bacterial cultures (Dalgaard *et al*., 1994). A third-order polynomial was obtained by fitting a curve to the data (Figure 1A). This function has been used in all our subsequent experiments to transform the observed OD values to OD values that are corrected for the non-linearity (Figure. 1B) before any further quantitative analysis of the growth curves.

General growth characteristics of yeast microcultivation

Shaking is not adequate to provide fully homogenous dispersion of cells in this microcultivation system, and some degree of cell sedimentation can be visually observed in the wells. In addition, we found the mode of shaking to be critical; constant shaking resulted in accumulation of cells at the periphery of, or as centrally located ridges in, the wells and subsequent atypical and non-reproducible growth curves even at the highest shaking intensity (Figure 2A–C). Alternating shaking (60 s) and resting (60 s; this is the shortest possible setting in the apparatus for non-shaking periods) turned out to be a solution to this problem and to provide normal growth curves (Figure 2D). This mode of shaking was used in all further experiments. The frequency of non-typical growth curves was also strongly dependent on the yeast strain; while strains like FY1679 (Figure 2D), BY, CEN.PK2 and W303 behaved neatly and provided good growth curves with alternating shaking (atypical growth curves for less than 1% of the wells); we could not obtain this for a strain like Sigma1278b, which always resulted in poor results from cellular aggregation. An algorithm was devised for the analysis of the growth parameters length of lag phase, doubling time and net increment in OD until stationary phase (see Materials and methods), designed to handle, in a robust way, even the occasional atypical growth

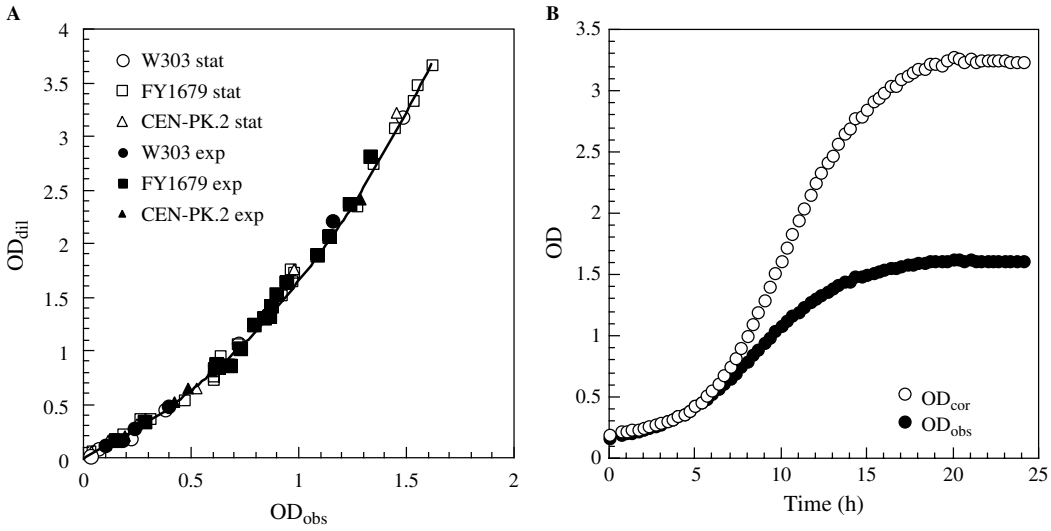

Figure 1. Correction strategy for the non-linearity of the optical recording at higher cell densities. (A) Optical recording of yeast cells in the microplate reader plotted as the relation between diluted and non-diluted cultures. The relation was tested for three different haploids from strains W303, CEN-PK.2 and FY1679 harvested at two growth phases [exponential phase (exp) and stationary phase (stat)]. An overnight stationary phase culture (E-flask) and an exponentially growing microplate culture of three different yeast laboratory strains were serially diluted and the optical density of the whole dilution series was measured in the microplate reader. The estimated OD (OD_{dil}) was calculated from OD_{obs} × dilution factor, where OD_{obs} stands for the OD read-out in the microplate reader (450–580 nm). The fitted third-order polynomial curve describe the function for corrected OD: $OD_{cor} = OD_{obs} + 0.449(OD_{obs})^2 + 0.191(OD_{obs})^3$. (B) Growth data obtained during microcultivation (OD_{obs}) is displayed together with the corrected growth data (OD_{cor}) by the use of the polynomial function indicated in A)

curves. In particular, it is important to notice that no value in net OD increment in the stationary phase was given unless a clear plateau was achieved.

An additional concern was a potentially atypical growth behaviour of cultures in the microplate. We compared growth characteristics between microplate cultivation (350 µl medium) and E-flask cultivation (10 ml medium in 125 ml E-flask) at different levels of salinity. The growth curves from microplate cultivation in saline media displayed normal salt dependence; the higher the salinity, the longer the lag-phase, the slower the rate of growth and the lower the stationary phase OD increment (Figure 3A). These characteristics of salt growth can be rationalized in a physiological and molecular context (Blomberg and Adler, 1992; Hohmann, 1997). However, even if the growth curves generated during growth in microplates exhibited qualitative similarities to normal batch cultivation, it was of interest to manifest not too great quantitative discrepancies. The doubling times obtained at different salinities were highly similar between the two growth systems (Figure 3B). The stationary

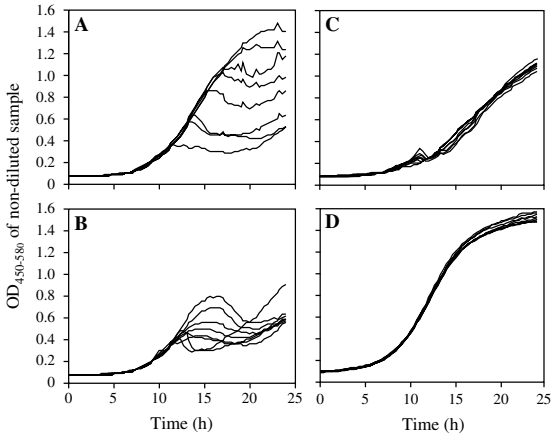

Figure 2. The influence from shaking intensity and shaking intervals on the obtained growth curves for strain FY1679 during growth in control medium. In each part (A–D) of the figure, 10 individual growth curves are displayed obtained from inoculation of 10 different wells, containing the standard growth medium (control medium), with the same inoculation culture. In these examples OD_{obs} has not been corrected to OD_{cor}. (A) low-intensity shaking; (B) medium-intensity shaking; (C) high-intensity shaking; and (D) high-intensity shaking in 60 s intervals with 60 s intermittent resting

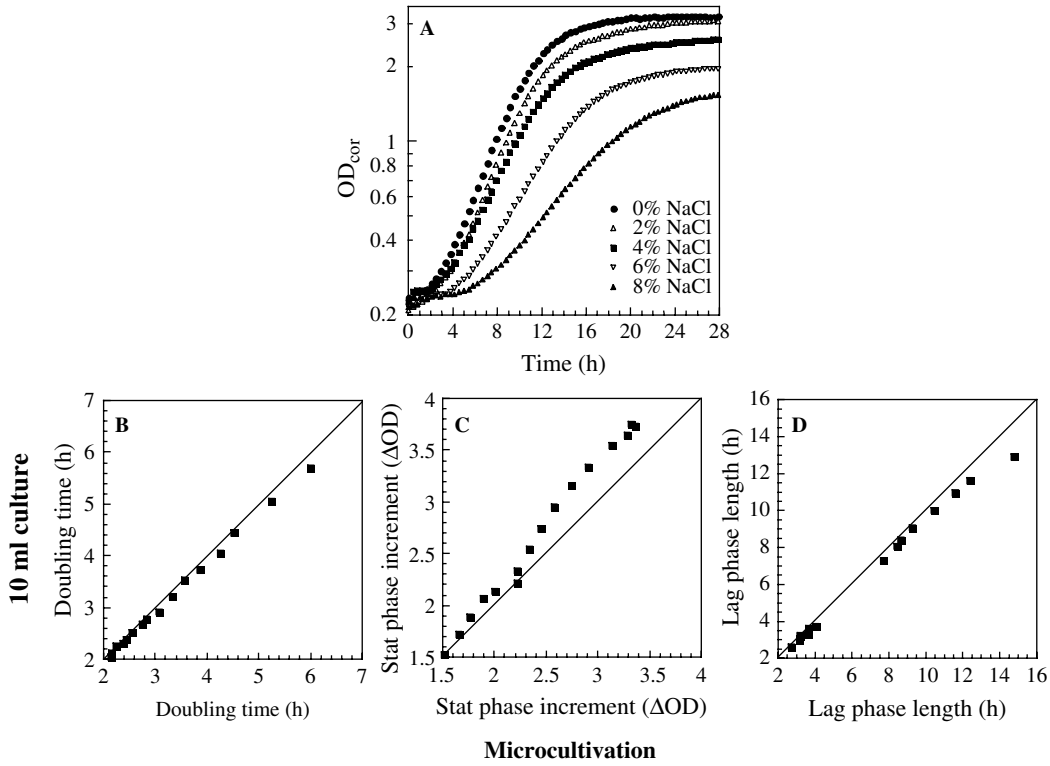

Figure 3. Correlation between growth parameters obtained during microcultivation and in 10 ml cultures (150 ml E-flask on a rotary shaker). The test was performed at 16 different salinities [0–8% (w/v) NaCl] with the same inoculation culture in both cases. (A) Growth data from microcultivation for five selected salinities in the range 0–8% (w/v) NaCl. OD_{obs} has been corrected to OD_{cor}. (B, C and D) Comparison of (B) doubling times, (C) stationary phase OD increments and (D) lengths of the lag phase between the two scales of cultivation. The line in (B), (C) and (D) indicates the 1 : 1 relation

phase OD increment also displayed a good correlation especially above roughly 5% NaCl (OD increment values < 2.4; Figure 3C), while at low salinity (OD increment values > 2.4) a somewhat lower stationary phase OD increment was consistently observed from growth in microplates. This we believe to be the result of oxygen limitations under growth in microplates; a more pronounced fermentative metabolism would be apparent, resulting in lower stationary phase cell density values. This indicates that this device might not be suitable for studies of fully respiratory growth, which is further supported by extremely slow growth when ethanol is supplied as the sole carbon and energy source (data not shown). Also the lag phase displayed a good fit between the two culture set-ups (Figure 3D). However, in spite of attempts to standardize the starter cultures we could not at this stage get a good reproducibility in the estimation of the length of the lag phase between days.

Protein expression is a sensitive reporter for changes in cellular physiology between different growth conditions. Differences in protein expression between microcultivation and E-flask cultivation were globally analysed by 2D electrophoresis separation and subsequent quantitative image analysis (Figure 4). The most abundant 730 protein spots were matched between all gels to allow for a more detailed quantitative analysis. Most proteins did not exhibit apparent changes in expression; however, it was found that 161 of the matched proteins exhibited statistically significant [Student's t test ($p < 0.05$) on log-transformed values] and a more than two-fold change in expression (up or down). Roughly half of the responding proteins altered expression by less than three-fold, while 17 proteins altered expression by at least a factor of 10; induction as a result of microcultivation was apparent for 15 of the proteins in this class of highly responding proteins. Among the more

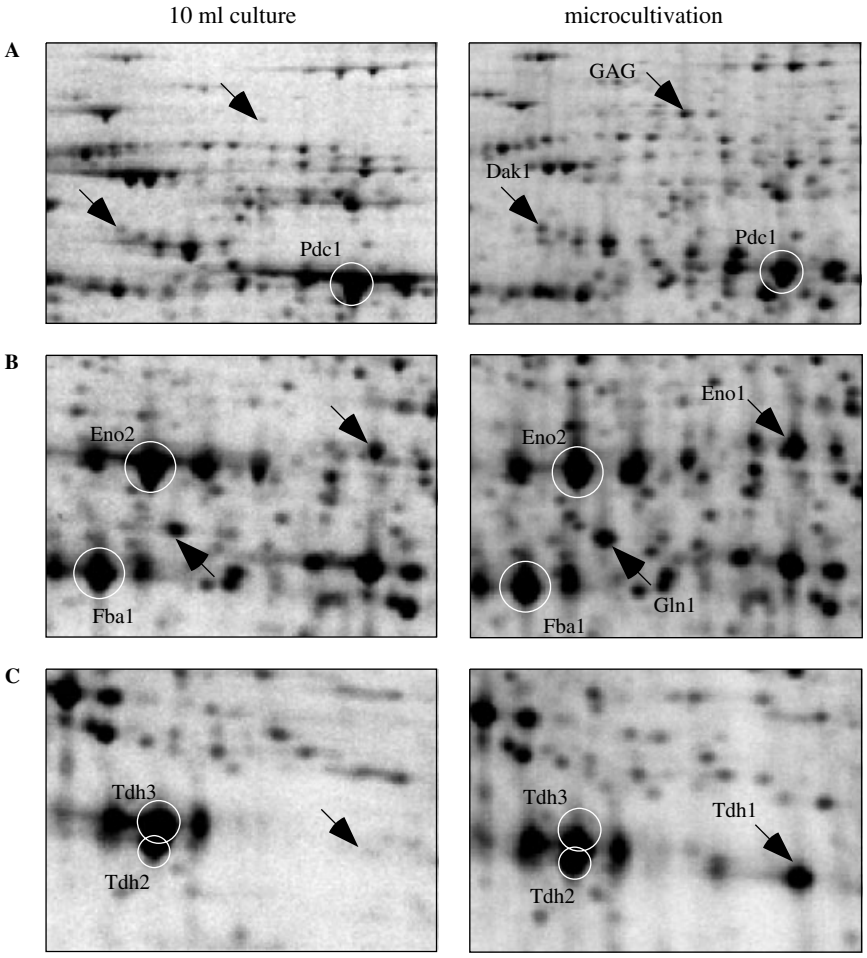

Figure 4. 2D–PAGE gel from ^{35}S-methionine-labelled cellular extract (YPH500) during microcultivation. Arrows indicate proteins where expression is higher during microcultivation. Some proteins with known identity has been indicated. For a complete coverage of the identified proteins in the 2D pattern, see **http://yeast-2DPAGE.gmm.gu.se**

moderately altered proteins were three members of the proposed glycerol cycle, Gpd1p, Gpp2p and Dak1p (Table 1), which are induced during osmotic dehydration (Blomberg, 2000) and by other stress treatments (Gasch *et al.*, 2000). The list of proteins upregulated during microcultivation (Table 1) displayed a number of other stress-related genes, such as Ctt1p, Hxk1p and Eno1p (Figure 4B). The minor isoform of glyceraldehyde-3-phosphate dehydrogenase, Tdh1p, exhibited in this study highly increased expression during microcultivation, while the two more dominant isoforms, Tdh2p and Tdh3p, did not alter expression (Figure 4C). A surprising finding was that the RNA L-A virus coat protein GAG was induced about 10-fold during microcultivation (Table 1, Figure 4A). Among the proteins that displayed decreased expression we repeatedly found protein components involved in protein synthesis (Table 1); this is clearly the case for ribosomal protein Rpl0Ap and the translational elongation factor Tef1p. In addition, two of the functionally less well-characterized proteins encoded by *YMR116c/BEL1* and *YKL056c* have been linked to protein synthesis, and both these proteins decreased in expression during microcultivation.

Screens in environmental arrays

To test the applicability of this microplate based methodology in phenotypic profiling, we performed a screen on MATα haploids of three laboratory yeast strains, FY1679, W303 and CEN-PK.2.

Table 1. Previously identified proteins in the yeast 2D–PAGE pattern that in this analysis displayed significant ($p < 0.05$) and at least two-fold differences in expression during growth in microplates compared to normal laboratory scale cultivation in 10 ml medium in E-flasks (strain YPH500). Average ppm values of duplicate independent experiments are displayed

Protein name	Micro-cultivation	10 ml E-flask	*n*-Fold increase
Induction during microcultivation			
Tdh1	11416	169	67
Isoform L-A virusprotein, GAG	1059	55	18
Isoform L-A virusprotein, GAG	198	17	11
Isoform L-A virusprotein, GAG	185	25	7
Ctt1	321	56	5
Tuf1	925	180	5
Eno1	12950	2983	4
Gpp2	143	39	3
Hxk1	1941	627	3
Gpd1	559	198	2
Pgi1	3254	1376	2
Tal1	1731	757	2
Dak1	533	235	2
Act1	11211	5156	2
Gln1	4890	2264	2
Rnr4	1474	888	2
Repression during microcultivation			
Ymr116c	2636	10719	4
RplA0	1444	4381	3
Gpp1	310	894	2
Ykl056c	3472	8987	2
Sam 1	1135	2658	2
Lys9	732	1702	2
Sod1	1198	2752	2
Tef1	18113	33009	2

These haploid laboratory strains were tested for quantitative growth differences in 98 different environments. Environments were selected as the control medium (synthetic defined medium with glucose as carbon and energy source) with and without either of 33 different chemicals with known inhibitory action on yeast growth, where all but two agents were administered at three different concentrations — low, medium and high. For a majority of the chemicals, the selected concentration range provided concentration-dependent differences in rate of growth (Figure 5). The rate of growth and the efficiency of growth (the latter reflected in the stationary phase OD increment; however, see Discussion for further treatment about the interpretation) are principally independent variables reflecting strictly different aspects of cell physiology. The algorithm was designed not to include any values for cultures that had not reached stationary phase of growth. Comparing the doubling times and stationary phase OD increment values it was clear that these two variables constituted different growth indicators, e.g. at the highest concentration of the translational inhibitor cycloheximide the doubling time about doubled compared to the control for strain FY1679 (Figure 5); however, no effect on stationary phase OD increment values were observed (data not shown).

Reproducibility

Standard deviations from two independent experiments performed on two different days (error bars indicated in Figure 5) were low and revealed that the reproducibility was high. However, the standard deviation can vary slightly between different inhibitors and was also found to be generally larger for longer doubling times. The average coefficient of variation for doubling time or stationary phase OD increment for all three strains under the 100 conditions was 11% and 9%, respectively (independent experiments on different days; duplicate runs; a total of 600 growth curves). However, the reproducibility of the length of the lag phase was not as good; average coefficient of variation 23%.

Profiling by phenotypic index

For each of the 97 specific environmental conditions, the impact on growth for a particular strain was related to growth in the control medium (in total three control wells/microplate). The estimated environmental coefficients for rate of growth (EC_{rate}) and for stationary phase OD increment ($EC_{stationary}$) thus normalizes for basal differences in growth capacity between strains and specifically expresses the fractional impact on the growth variables rate or OD increment in that particular environmental condition. In this case the three strains grew in the control medium with about the same doubling time (range 2.1–2.5 h) and to roughly the same stationary phase OD increment (range 2.75–3.1 OD units), and thus the effect from normalization will in this case not be so drastic. However, the strategy of calculating EC_{rate} and

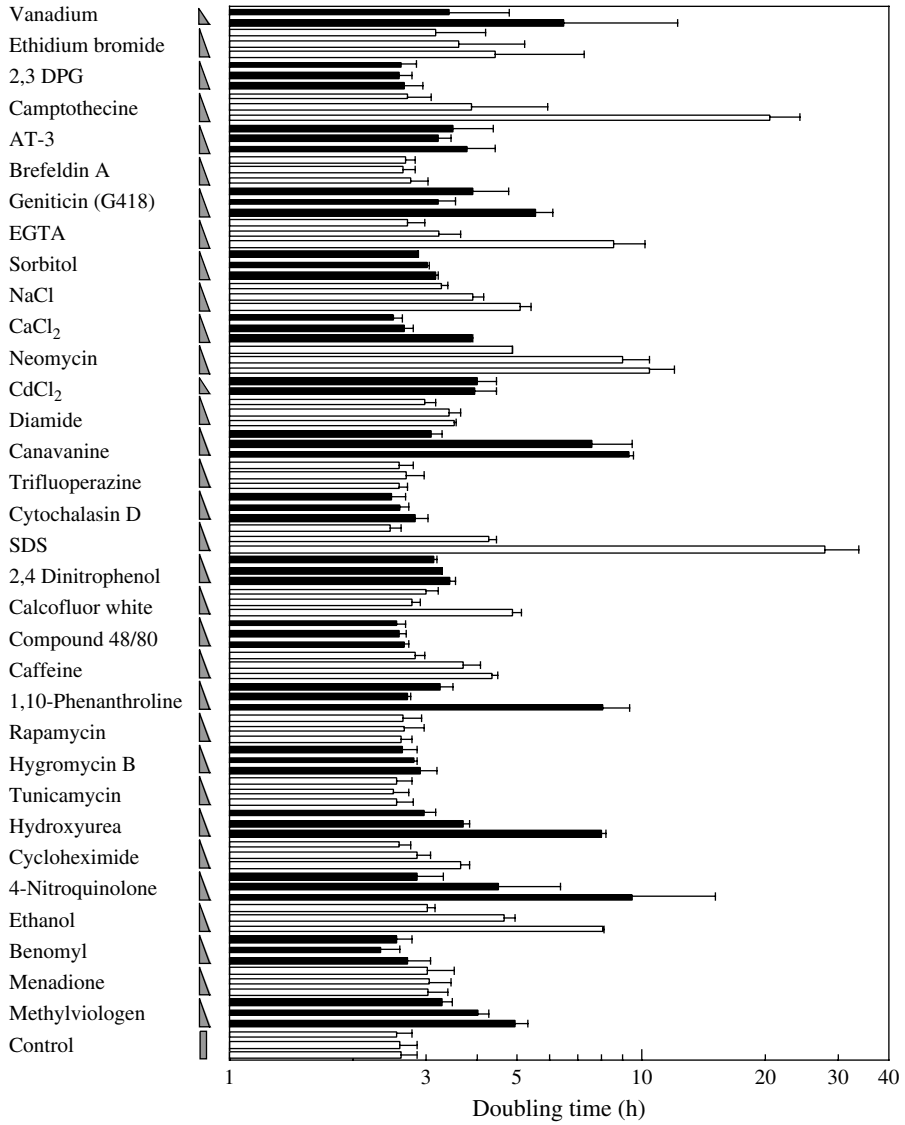

Figure 5. Doubling times for the 98 different growth conditions for strain FY1679. Wedges along the names of the different chemicals indicate differences in concentration (low to high). For actual values of the different inhibitors, see Materials and methods. Indicated values are averages and error bars represent SD from two independent experiments (different days)

$EC_{stationary}$ makes the data treatment more generally applicable, e.g. when deletion mutants are to be analysed where the overall rate of proliferation even in control medium is strongly hampered.

In addition, to be able to easily visualize the difference in quantitative phenotypes between different strains (especially valid when comparing deletion mutants and the corresponding wild-type), a phenotypic index was calculated as the ratio between the corresponding environmental coefficients for a particular strain s ($EC_{rate,s}$ and $EC_{stationary,s}$) and the values for a reference strain rf ($EC_{rate,rf}$ and $EC_{stationary,rf}$). In this study, strain FY1679 was arbitrarily chosen as the reference. The phenotypic indexes for rate of growth (phenotypic $index_{rate}$) were in this way calculated for the 98 different environments for the strains W303 and CEN.PK2 (Figure 6). A value of the phenotypic $index_{rate}$ <1 indicates a greater growth defect compared to the reference strain FY1679. The phenotypic index thus links some specific property of the strain to that particular growth

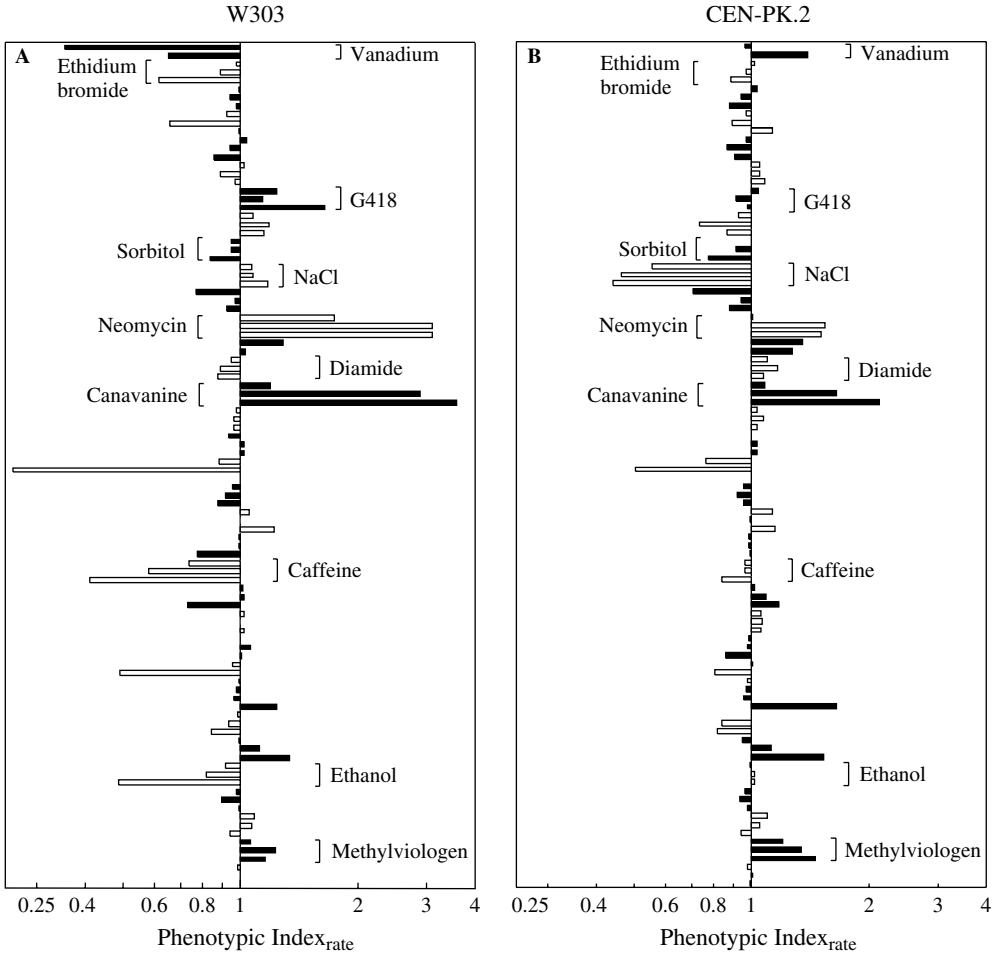

Figure 6. Phenotypic profiling in the environmental arrays for differences in phenotypic index$_{rate}$, for strains W303 (A) and CEN-PK.2. (B) in relation to strain FY1679. The order of the chemicals on the *y* axis is the same as in Figure 4. Conditions where clear and roughly concentration dependent changes in phenotypic index$_{rate}$ can be observed are indicated

inhibitor. The strains displayed clearly different phenotypic index$_{rate}$ under many of the conditions tested and the overall profiles obtained were unique and provided a quantitative phenotypic fingerprint for each strain.

The W303 strain was found most sensitive when comparing the 13 inhibitors that produced clear alterations in phenotypic index for at least two of the three concentrations; the five inhibitors for which strain W303 was most sensitive were vanadate, ethidiumbromide, diamide, caffeine and ethanol (Figure 6). The strain CEN-PK.2 was highly sensitive under conditions of osmotic stress. This was most apparent when osmotic stress was administered by NaCl addition, i.e. a phenotypic index$_{rate}$ of about 0.55 at the highest concentration. The osmolarity of the highest concentration of sorbitol is about equal to the lowest concentration of NaCl, which indicates that this strain has problems with NaCl that are not exclusively linked to the osmotic component of NaCl stress. Both W303 and CEN-PK.2 displayed high phenotypic index$_{rate}$ values in both neomycin and canavanine, indicating that these compounds have a greater effect on strain FY1679.

Comparison of phenotypic index$_{rate}$ and phenotypic index$_{stationary}$

The phenotypic index$_{stationary}$ was calculated in principle by the same overall procedure as for phenotypic index$_{rate}$ but now considering the

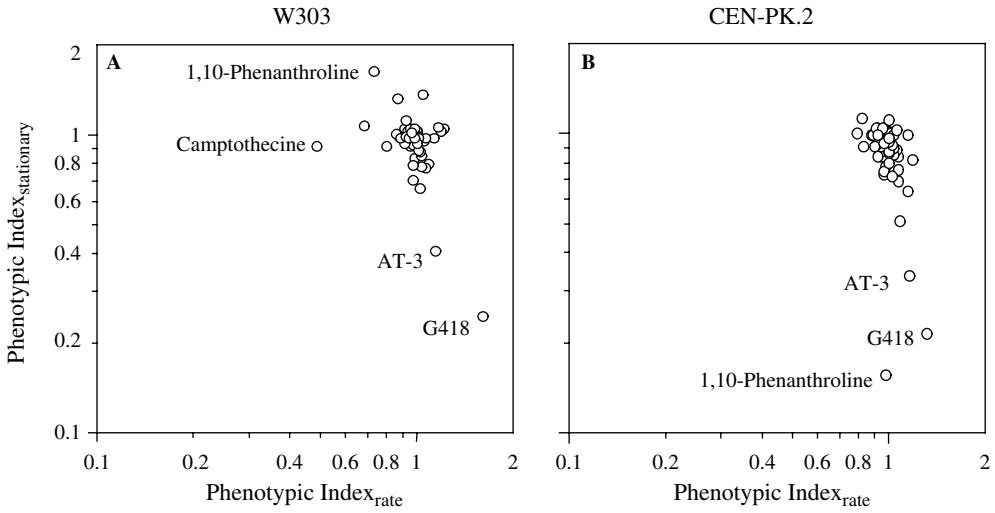

Figure 7. The relation between phenotypic index$_{rate}$ and phenotypic index$_{stationary}$ from phenotypic profiling in the environmental arrays. Care has been take only to include stationary phase OD increment values that displayed a true growth plateau (constant OD values for at least five consecutive recordings). (A) W303 and (B) CEN-PK.2. Some conditions that clearly revealed differences in the values for phenotypic index$_{rate}$ and phenotypic index$_{stationary}$ have been indicated

$EC_{stationary}$ values. Strain-specific differences in physiology that was exclusively revealed by analysis of OD increment in stationary phase was apparent from plots of phenotypic index$_{rate}$ vs. phenotypic index$_{stationary}$ (Figure 7). One clear example of this is the effect of the chelator 1,10-phenanthroline, with high preference for zinc and iron, which showed a large effect on the OD increment value obtained while hardly affecting the rate of growth when comparing CEN-PK.2 and FY1679; CEN-PK.2 displayed a reduction in phenotypic index$_{stationary}$ to 0.15 at the highest concentration. The inhibitor AT-3 (1,2,4-aminotriazole), which is a competitive inhibitor of histidin biosynthesis, caused a reduction in phenotypic index$_{stationary}$ for both CEN-PK.2 and W303 compared to the FY1679 strain. Both these strains were also more influenced by addition of the translational inhibitor G418 (geneticin) reflected in values of phenotypic index$_{stationary} < 1$. In the case of W303 the opposite effect was observed when the rate of growth was compared during geneticin growth; this strain exhibited a phenotypic index$_{rate}$ value of about 1.6 at the highest concentration (Figure 7). Further indications of differences in the response was seen in W303 during growth with the inhibitor camptothecin; no effect was found on phenotypic index$_{stationary}$ while phenotypic index$_{rate}$ was roughly 0.5 (Figure 7).

Discussion

Physiology of microcultivated yeast

It is clear from our data that the yeast *S. cerevisiae* can be cultivated in a microplate format at a media volume of 350 μl and retain relevant growth characteristics, both for high and low rates of proliferation. We thus propose this to be a valuable procedure for large-scale screens of mutant phenotypes. However, changes in scale of cultivation usually lead to some change in cell physiology. In the present study we found a consistently lower stationary phase value during microcultivation. This might reflect slight oxygen limitation during these scaled-down conditions, resulting in less respiration and thus less efficient utilization of the carbon and energy source. Low supply of oxygen was also indicated from the poor growth on the respiratory carbon source ethanol. Altered physiology during microcultivation was revealed by increased production of the glyceraldehyde-3-phospate dehydrogenase isoform Tdh1p. Increased production of Tdh1p has been linked to high internal concentration of NADH (Valadi H, Månsson Å, Norbeck J *et al*., Unpublished manuscript). We thus believe that microcultivation, with a limited access of oxygen, will have similar impact on the internal redox balance, and thus triggers the expression of *TDH1*. Microcultivation also affected the expression of

other proteins previously shown to be involved in the cellular stress responses. Whatever the stress encountered during these conditions of microcultivation, there were no drastic effects on the rate of proliferation, indicating that these protein responses do not link to hampered growth *per se*. A surprise was the induced replication of the L-A virus, as indicated by the increased expression of the coat protein GAG. The regulation of this virus is well understood at the level of molecular mechanisms involved (Benard *et al*., 1999; Wickner, 1996); however, almost nothing is known about the external factors that triggers its replication (B. Wickner, personal communication). In summary, it should be expected that for certain strain behaviours differences will be encountered between micro- and E-flask cultivation, which has to be kept in mind when our data is compared to other types of phenotypic analyses.

Phenotypic profiling of laboratory yeast strains

A number of laboratory strains are in use in yeast research. Many of these strains are related to the S288C strain (Mortimer and Johnston, 1986), which is the case for the FY1679 strain (Thierry *et al*., 1990). The W303 strain stems from a strain W301-18A, a descendent of X2180 that was derived from S288C by self-diploidization; however, some other strains of more or less known origin also contributed to W301-18A (Rogowska-Wrzesinska *et al*., 2001). The origin of strain CEN-PK.2 is from a number of crosses between strain ENY.WA-1A and MC996 (P. Kotter, personal communication). Genotypic differences have the potential to result in different phenotypic traits and in the present analysis we clearly show that these different laboratory strains have rather different phenotypes; the overall quantitative phenotypic profile for the environmental array of almost 100 different growth conditions provided a highly selective fingerprint for each strain. This is the first published large-scale comparison of marginal growth phenotypes in these strains and most of the differences would not have been detected by qualitative screens for growth on plates. We also show that some phenotypic differences were encountered only when screening for putative changes in efficiency of growth, scored as differences in stationary phase OD increment values, which highlights the importance of analysis of changes in different variables of the growth curve. In an earlier investigation about differences in the proteome of these three strains, FY1679 and W303 were most similar to each other (Rogowska-Wrzesinska *et al*., 2001). Differences between the three strains have also been reported for the lipid content, where the FY1679 strain in particular stands out with lower sterol and triacylglycerol content and an unusual fatty acid composition (Daum *et al*., 1999). Different genetic backgrounds might cause problems in the interpretation of the physiological consequences of gene deletions (Bilsland *et al*., 1998; Duenas *et al*., 1999) or alterations in gene expression from external factors (Norbeck and Blomberg, 2000). These reported examples and our phenotypic analysis, which clearly display strain differences in the response to external factors, highlight the care with which biological information and conclusions should be transmitted between different yeast strains.

Quantitative contra qualitative growth phenotypes

The importance of providing refined quantitative phenotypic information about deletion mutants is supported by the analysis of the marginal fitness contribution of non-essential genes in yeast (Thatcher *et al*., 1998). It was estimated that about 60% of the deletion mutants will exhibit marginal reduction in fitness. Thus, if phenotypic information is to be provided for most deletion strains, quantitative screens have to be implemented. However, for 20% of the mutants no change in marginal fitness during cultivation in rich medium was observed (Thatcher *et al*., 1998). We believe that by extending the analysis to more conditions, as in these environmental arrays, indications of marginal but significant growth phenotypes will be provided for almost all deletion strains. In addition, we advocate analysis of mutant physiology to be performed in liquid media, since the mutant phenotype scored on an agar plate is a combined result of possible changes of the parameters length of the lag phase, rate of growth and growth efficiency (and maybe even other factors). In the analysis of marginal fitness effects by Thatcher *et al*. (1998), the measured differences between strains are really the sum of alterations in any of these three growth parameters, together with additional features such as production of inhibitors and competitions for nutrients.

Relative fitness is also measured in the screening of mixed large populations by utilizing the barcoded mutant collection and microarray analysis (Winzeler *et al*., 1999) or the PCR based quantification of strain fractions (Baganz *et al*., 1998; Smith *et al*., 1996). Analysis of pools of mutants is a promising procedure in large-scale mutant characterization for fitness effects. However, it might not be well suited for the analysis of strain-specific phenotypic traits that are to be interpreted as gene-by-environment interactions linked to features of cellular physiology, since growth might be influenced by other strains in the population. We have found indications of induced replication of L-A virus as a result of specific gene deletions (Warringer and Blomberg, unpublished data). Replication of L-A virus is mostly accompanied by killer toxin production and strains expressing the toxin are also resistant to its action (Wickner, 1996). Thus, strain-specific expression of the killer toxin, which could restrict growth of other strains, is one example of a factor that hamper interpretation of growth data from mixed population of mutants. We thus advocate the analysis of strains in isolation.

We also introduce the concepts of phenotypic $\text{index}_{\text{rate}}$ and phenotypic $\text{index}_{\text{stationary}}$ as physiologically relevant phenotypic indicators in the characterization of yeast strains and we here show that these can be reproducibly measured. An important observation is that these features of a strain appear in some instances to be independent variables and thus a deletion mutant could be expected to reveal a phenotype on any of these. We predict the interpretation of recorded phenotypes on deletion mutants to benefit greatly from the discrimination between rate and OD increment effects. However, it should be stressed in this context that the stationary phase OD increment should be viewed with some caution as an indicator of efficiency of growth. First, the relation between the biomass and the OD measured is known to be dependent on a number of factors and can differ quite substantially between different strains. Second, we do not know if the end of the growth phase is always the result of complete utilization of the carbon source glucose.

Mutant features can provide insight to the cellular role or molecular function of a gene by guilt by association via clustering of obtained result (Ross-Macdonald *et al*., 1999), a strategy that is frequently applied to expression data (Eisen *et al*., 1998). We are convinced that clustering based on data concerning quantitative alterations in phenotypic index will provide high-quality biological information. The automated system presented in this study will thus be used in our laboratory as a platform for large scale screening for quantitative changes in growth phenotypes, during a large number of environmental conditions, in the collection of deletion mutants in the BY background (Brachmann *et al*., 1998).

Acknowledgement

The financial support from the Foundation for Strategic Research (SSF) is highly appreciated. We also express our gratitude to J. Norbeck for providing the haploid yeast strains. Comments from colleagues have been instrumental during the course of this work, where we would like, in particular, to thank L. Adler, O. Nerman and E. Ericson for valuable comments on the manuscript.

References

Baganz F, Hayes A, Farquhar R, Butler PR, Gardner DCJ, Oliver SG. 1998. Quantitative analysis of yeast gene function using competition experiments in continuous culture. *Yeast* **14**: 1417–1427.

Benard L, Carroll K, Valle RC, Masison DC, Wickner RB. 1999. The ski7 antiviral protein is an EF1-α homolog that blocks expression of non-Poly(A) mRNA in *Saccharomyces cerevisiae*. *J Virol* **73**: 2893–2900.

Bianchi MM, Ngo S, Vandenbol M, *et al*. 2001. Large-scale phenotypic analysis reveals identical contributions to cell functions of known and unknown yeast genes. *Yeast* **18**: 1397–1412.

Bilsland E, Dahlén M, Sunnerhagen P. 1998. Genomic disruption of six budding yeast genes gives one drastic example of phenotype strain-dependence. *Yeast* **14**: 655–664.

Blomberg A. 2000. Metabolic surprises in *Saccharomyces cerevisiae* during adaptation to saline conditions: questions, some answers and a model. *FEMS Microbiol Lett* **182**: 1–8.

Blomberg A, Adler L. 1992. Physiology of osmotolerance in fungi. *Adv Microbial Phys* **33**: 145–212.

Blomberg A, Blomberg L, Norbeck J, *et al*. 1995. Interlaboratory reproducability of yeast protein patterns analyzed by immobilized pH gradient two-dimensional electrophoresis. *Electrophoresis* **16**: 1935–1945.

Brachmann CB, Davies A, Cost GJ, *et al*. 1998. Designer deletion strains derived from *Saccharomyces cerevisiae* S288C: a useful set of strains and plasmids for PCR-mediated gene disruption and other applications. *Yeast* **14**: 115–132.

Chan TF, Carvalho J, Riles L, Zheng XF. 2000. A chemical genomics approach toward understanding the global functions of the target of rapamycin protein (TOR). *Proc Natl Acad Sci USA* **97**: 13 227–13 232.

Cowen LE, Kohn LM, Anderson JB. 2001. Divergence in fitness and evolution of drug resistance in experimental populations of *Candida albicans*. *J Bacteriol* **183**: 2971–2978.

Dalgaard P, Ross T, Kamperman L, Neumeyer K, McMeekin TA. 1994. Estimation of bacterial growth rates from turbidimetric and viable count data. *Int J Food Microbiol* **23**: 391–404.

Daum G, Tuller G, Nemec T, *et al*. 1999. Systematic analysis of yeast strains with possible defects in lipid metabolism. *Yeast* **15**: 601–614.

Duenas E, Vazquez de Aldana CR, de Cos T, Castro C, Henar Valdivieso M. 1999. Generation of null alleles for the functional analysis of six genes from the right arm of *Saccharomyces cerevisiae* chromosome II. *Yeast* **15**: 615–623.

Dwight SS, Harris MA, Dolinski K, *et al*. 2002. *Saccharomyces* Genome Database (SGD) provides secondary gene annotation using the Gene Ontology (GO). *Nucleic Acids Res* **30**: 69–72.

Eisen MB, Spellman PT, Brown PO, Botstein D. 1998. Cluster analysis and display of genome-wide expression patterns. *Proc Natl Acad Sci USA* **95**: 14 863–14 868.

Gasch AP, Spellman PT, Kao CM, *et al*. 2000. Genomic expression programs in the response of yeast cells to environmental changes. *Mol Biol Cell* **11**: 4241–4257.

Giaever G, Chu AM, Ni L, *et al*. 2002. Functional profiling of the *Saccharomyces cerevisiae* genome. *Nature* **418**: 387–391.

Hajji K, Clotet J, Arino J. 1999. Disruption and phenotypic analysis of seven ORFs from the left arm of chromosome XV of *Saccharomyces cerevisiae*. *Yeast* **15**: 435–441.

Hirsh AE, Fraser HB. 2001. Protein dispensability and rate of evolution. *Nature* **411**: 1046–1049.

Hohmann S. 1997. Shaping up: the response of yeast to osmotic stress. In *Yeast Stress Responses*, Hohmann S, Mager WH (eds). Springer: Berlin; 101–146.

Lafuente MJ, Gancedo C. 1999. Disruption and basic functional analysis of six novel ORFs of chromosome XV from *Saccharomyces cerevisiae*. *Yeast* **15**: 935–943.

Lewis S, Ashburner M, Reese MG. 2000. Annotating eukaryote genomes. *Curr Opin Struct Biol* **10**: 349–354.

Mortimer RK, Johnston JR. 1986. Geneology of principal strains of the yeast genetic stock centre. *Genetics* **113**: 35–43.

Norbeck J, Blomberg A. 1997. Two-dimensional electrophoretic separation of yeast proteins using a non-linear wide range (pH 3–10) immobilized pH gradient in the first dimension; reproducability and evidence for isoelectric focusing of alkaline (pI > 7) proteins. *Yeast* **13**: 529–539.

Norbeck J, Blomberg A. 2000. The level of cAMP dependent protein kinase A activity strongly affects osmotolerance and osmo-instigated gene expression changes in *Saccharomyces cerevisiae*. *Yeast* **16**: 121–137.

Oliver SG. 1997. From gene to screen with yeast. *Curr Opin Genet Dev* **7**: 405–409.

Rieger K-J, Orlowska G, Kaniak A, Coppee J-Y, Aljinovic G, Slonimski PP. 1999a. Large-scale phenotypic analysis in microtitre plates of mutants with deleted open reading frames from yeast chromosome III: key-step between genomic sequencing and protein function. *Methods Microbiol* **28**: 205–227.

Rieger KJ, El-Alama M, Stein G, Bradshaw C, Slonimski PP, Maundrell K. 1999b. Chemotyping of yeast mutants using robotics. *Yeast* **15**: 973–986.

Rieger KJ, Kaniak A, Coppee JY, *et al*. 1997. Large-scale phenotypic analysis — the pilot project on yeast chromosome III. *Yeast* **13**: 1547–1562.

Rodriguez-Navarro S, Estruch F, Perez-Ortin JE. 1999. Functional analysis of 12 ORFs from *Saccharomyces cerevisiae* chromosome II. *Yeast* **15**: 913–919.

Rogowska-Wrzesinska A, Mose-Larsen P, Blomberg A, *et al*. 2001. Comparison of proteome of three yeast wild-type strains: CEN.PK2, FY1679 and W303. *Comp Funct Genom* **2**: 207–225.

Ross-Macdonald P, Coelho PS, Roemer T, *et al*. 1999. Large-scale analysis of the yeast genome by transposon tagging and gene disruption. *Nature* **402**: 413–418.

Smith V, Chou KN, Lashakari D, Botstein D, Brown PO. 1996. Functional analysis of the genes of yeast chromosome V by genetic footprinting. *Science* **274**: 2069–2074.

Steinmetz LM, Scharfe C, Deutschbauer AM, *et al*. 2002. Systematic screen for human disease genes in yeast. *Nature Genet* **31**: 400–404.

Thatcher JW, Shaw JM, Dickinson WJ. 1998. Marginal fitness contributions of non-essential genes in yeast. *Proc Natl Acad Sci USA* **95**: 253–257.

Thierry A, Fairhead C, Dujon B. 1990. The complete sequence of the 8.2 kb segment left of MAT on chromosome III reveals five ORFs, including a gene for a yeast ribokinase. *Yeast* **6**: 521–534.

Wickner RB. 1996. Double-stranded RNA viruses of *Saccharomyces cerevisiae*. *Microbiol Rev* **60**: 250–265.

Winzeler EA, Shoemaker DD, Astromoff A, *et al*. 1999. Functional characterization of the *S. cerevisiae* genome by gene deletion and parallel analysis. *Science* **285**: 901–906.

Wysocki R, Roganti T, Van Dyck E, de Kerchove D'Exaerde A, Foury F. 1999. Disruption and basic phenotypic analysis of 18 novel genes from the yeast *Saccharomyces cerevisiae*. *Yeast* **15**: 165–171.

Zuniga S, Boskovic J, Jimenez A, Ballesta JP, Remacha M. 1999. Disruption of six *Saccharomyces cerevisiae* novel genes and phenotypic analysis of the deletants. *Yeast* **15**: 945–953.

